The duration of near-peak metamorphism from diffusion modelling of garnet zoning

F. S. SPEAR

Department of Earth and Environmental Sciences, Rensselaer Polytechnic Institute, Troy, NY 12180, USA (spearf@rpi.edu)

ABSTRACT

Garnet in a staurolite–kyanite zone sample from central Vermont displays a bell-shaped Mn growth zoning with diffusional modification over the outer 100 μ m. The diffusion is driven by the prograde net transfer reaction garnet + chlorite = kyanite + biotite as is evidenced by a well-defined resorption zone on the rim. Analysis of the reaction history and resorbed garnet composition suggests that the peak temperature attained was 620–660 °C. Diffusional modelling of the rim diffusion provides an estimate of the duration of the metamorphic episode over which significant garnet diffusion occurs. The duration is a function of the assumed peak temperature and garnet diffusivities and range from a few hundred thousand years to a few million years. Such short durations require rapid tectonic burial and exhumation of relatively thin tectonic slices.

Key words: diffusion modelling; garnet zoning; metamorphic time-scales.

INTRODUCTION

Diffusion is thermally activated, so the maximum potential for diffusive transfer occurs at or near the maximum temperature experienced by a rock. Modelling zoning profiles produced by diffusion that occurred near the metamorphic peak therefore have the potential to constrain the duration of near-peak metamorphic conditions.

The efficacy of a mineral to experience diffusive transfer depends on the diffusivity of the element of interest (in temperature and time space) and the magnitude of the chemical gradient driving the diffusion. Diffusivities of Fe, Mg and Mn in garnet are appropriate for studies in medium to high-grade metamorphic rocks. Exchange reactions (e.g. Fe–Mg exchange between garnet and biotite) produce changing boundary conditions at the garnet rim that can drive diffusion, but the change with temperature is fairly modest so the diffusion profiles are often not well formed. Net transfer reactions, on the other hand, have respectably large T-X changes and can generate substantial composition gradients that can be measured with good precision (e.g. Spear, 2004).

This paper reports on the results of diffusion modelling of composition profiles on the rim of a garnet from the staurolite-kyanite zone in east-central Vermont. As discussed in detail below, the zoning is clearly the product of diffusive transfer accompanied by garnet resorption resulting from the near-peak prograde reaction garnet + chlorite = kyanite + biotite.

Modelling the chemical zoning in garnet is relatively straightforward and good fits between model and observed zoning have been produced. The greatest uncertainty, it turns out, is knowledge of the temperature at which diffusion occurs. In the present

study, the diffusion is constrained through phase equilibria analysis to have occurred near the metamorphic peak, so the challenge is to determine the peak conditions with as much certainty as possible. This paper presents the results of the diffusion modelling and associated uncertainties first, and then analyses the uncertainty in the peak metamorphic conditions and implications for the duration of the metamorphism.

METHODS

X-ray maps and chemical analyses were obtained using the Cameca SX-100 electron probe at Rensselaer Polytechnic Institute. The X-ray maps were collected as raw counts using a current of 40 nA and dwell time of 50 ms per pixel and were uncorrected for background or concentration. The Fe/(Fe+Mg) X-ray maps were calculated using a FORTRAN program written by the author using the raw counts for each pixel in the Fe and Mg X-ray maps. Quantitative analyses were performed using natural and synthetic minerals as standards and corrected for matrix effects using a ZAF routine.

Diffusion modelling was accomplished using two FORTRAN programs written by the author employing an explicit finite difference algorithm (e.g. Crank, 1975). Only the outer 1 mm of the garnet was modelled and a grid spacing $0.5 \mu m$ was used. Time increments were set so that the value of the dimensionless parameter $r = D\Delta t/\Delta x^2$ remained constant at 0.4. Initial conditions were the inferred garnet zoning immediately before commencement of resorption. The rim boundary of the garnet was changed linearly with increasing temperature to the measured concentration on the garnet rim. The interior boundary (towards the core of the garnet) was of fixed

composition. One program incorporated only Mn tracer diffusivity and the other invoked a fourcomponent diffusion model similar to that described by Spear & Florence (1992) and using the Lasaga (1979) approach to calculating interdiffusion coefficients with Mg as the dependent variable. Garnet diffusivities used were those published by Chakraborty & Ganguly (1992), although similar results are obtained using the models of Carlson (2006). A discussion of the choice of diffusion coefficients, and implications of uncertainties in down-temperature extrapolation of these data, is presented later. Models were run assuming several different peak temperatures each with different temperature-time histories until a good visual match was obtained. The initial temperature for each model was 25 °C below the peak temperature and it was assumed that all resorption occurred between this temperature and the peak temperature. Variations on the rate and temperature interval of resorption did not affect the final duration by more than ~5%. The models were terminated 100 °C below the peak temperature.

The phase equilibria analysis was done using the FORTRAN Program Gibbs written by the author using thermodynamic data from Spear & Pyle (2010). Thermobarometry results were calculated using the FORTRAN Program GTB (Spear *et al.*, 1991) and the calibrations of Hodges & Spear (1982) for garnet—biotite thermometry and GASP barometry.

SAMPLE CHARACTERISTICS

The sample investigated (TM-730) comes from the Devonian Gile Mountain Formation in the stauro-lite-kyanite zone in east-central Vermont (Fig. 1). The region is characterized by a single episode of Barrovian metamorphism that occurred during the Devonian Acadian Orogeny (Doll *et al.*, 1961; Thompson & Norton, 1968). The structural evolution involved early fold nappes followed by later doming (White & Jahns, 1950). Sample TM-730 is from an outcrop at the south end of the Strafford Dome (latitude: 43.75087, longitude: –72.39206). Menard & Spear (1993, 1994) reported peak conditions of 9–10 kbar at 575–600 °C and generally clockwise P-T paths in the vicinity of the Strafford Dome.

Sample TM-730 contains garnet + biotite + staurolite + kyanite + muscovite + quartz + plagioclase \pm ilmenite \pm rutile + graphite \pm chlorite. Chlorite only occurs locally as alteration of garnet or biotite and is interpreted to be retrograde. The fabric is dominated by a pervasive nappe-stage schistosity (S2 of Menard & Spear, 1994) (Fig. 2) and relicts of the beddingparallel S1 schistosity can be seen locally in microlithons. Garnet is subidioblatic and there exists a distinct and well-defined reaction zone around the margin of each garnet crystal (Fig. 3). The reaction zone in Fig. 3 is comprised of biotite + muscovite + quartz + plagioclase + kyanite and is up to 600 μ m

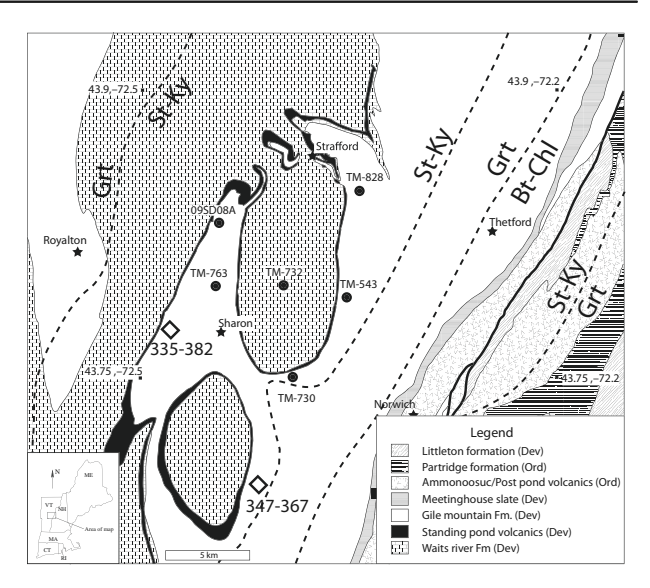


Fig. 1. Geological map of east-central Vermont after Doll *et al.* (1961) showing location of sample TM-730 (this study), samples from Spear *et al.* (2012) and metamorphic isograds. Diamonds show locations and ages of monazite from Wing *et al.* (2003). Inset shows location of map in central New England.

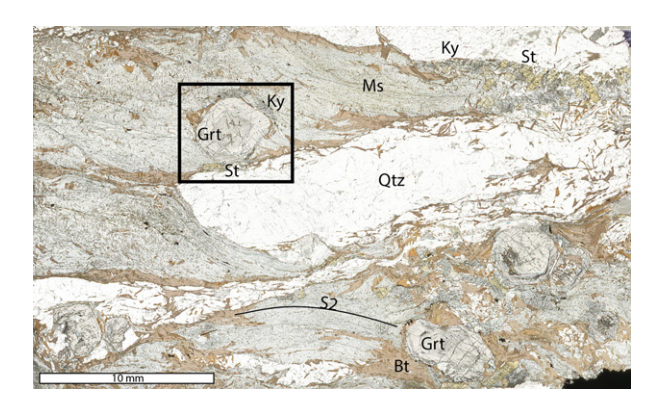


Fig. 2. Scan of thin section of sample TM-730. The label 'S2' identifies the dominant nappe stage foliation. Box shows location of Fig. 3a. Mineral abbreviations after Kretz (1983).

wide based on visual inspection of the change in rock texture and the occurrence of kyanite. This estimate of reaction zone width is also supported by mass balance calculations discussed below. The phases in the reaction zone represent a higher metamorphic grade than the garnet zone, and the reaction producing the reaction zone is inferred to be: garnet + chlorite + muscovite = kyanite (or staurolite) + biotite + quartz + plagioclase + H_2O .

CHEMICAL ZONING

Figures 4 and 5 are X-ray maps and a rim-to-core zoning traverse for the garnet under study. The zoning is typical of Barrovian garnet-zone crystals with

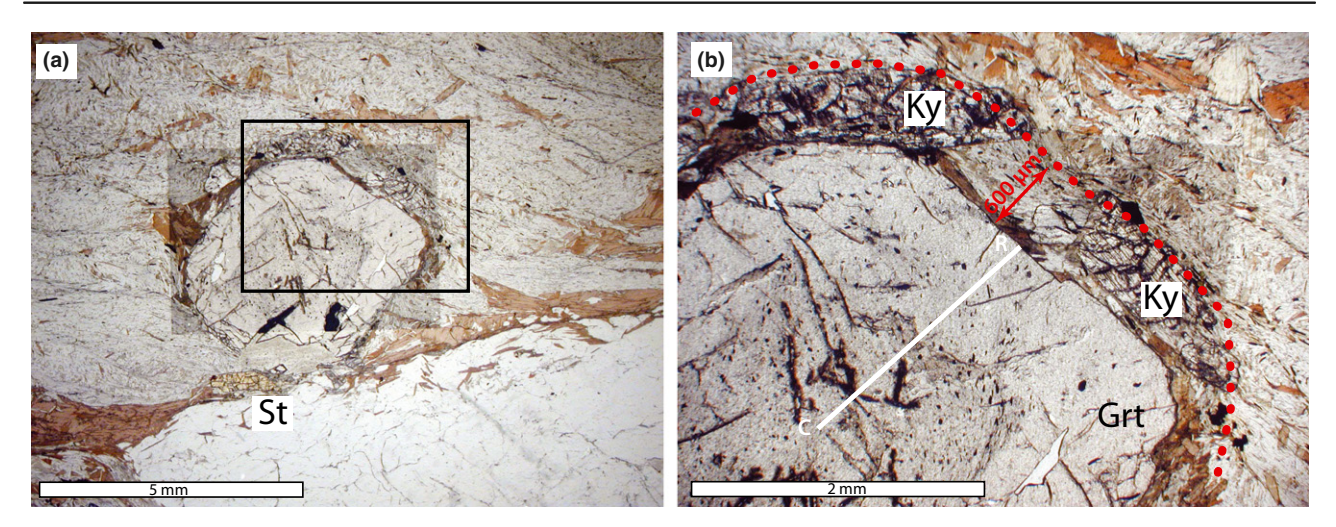


Fig. 3. (a) Photomicrograph of garnet from sample TM-730 analysed in this study. Box shows location of image in (b). (b) Closeup of garnet rim. Note reaction zone that is symmetrical around the rim of the garnet. Red dotted line shows maximum extent of reaction zone. White line labelled C-R shows location of electron probe traverse (Fig. 5). Inclusions in garnet core are pseudomorphs after clinozoisite. Grey shadow rectangle in both (a) and (b) is electron beam damage incurred during X-ray

 X_{Sps} decreasing from core to rim as a result of T-Xphase relations and Rayleigh fractionation (e.g. Hollister, 1966; Spear et al., 1990). Similarly, X_{Prp} increases, X_{Alm} increases then decreases and Fe/ (Fe+Mg) decreases monotonically from core to rim. $X_{\rm Grs}$ is constant at ~0.25 mole fraction in the core due to equilibrium with clinozoisite or epidote (e.g. Menard & Spear, 1993) and decreases to ~0.15 at the rim once all of the epidote is consumed.

The notable distinctive feature of the zoning is the dramatic change within 100 μ m of the rim. X_{Sps} increases as does Fe/(Fe+Mg), whereas X_{Prp} decreases. These changes are interpreted as resulting from diffusive exchange between the reaction zone and the garnet and are the focus of the diffusion modelling discussed in the next section.

DIFFUSION MODELLING

Tracer diffusion of Mn

Tracer diffusion of Mn into garnet will be considered first because it is conceptually simplest to visualize and the initial and boundary conditions are relatively well constrained. Applying Mn tracer diffusivity is also not a serious limitation as the concentration of Mn in the garnet rim is nearly that of a trace element. As shown below, the significant results of this study are equally well described by Mn tracer diffusion as by a four-component garnet diffusion model.

Initial conditions

It is inferred that prior to the onset of the formation of the reaction selvage, the garnet crystal was larger and continuously zoned through continuous reaction in the assemblage

$$chlorite + epidote + quartz + plagioclase \\ \pm \ muscovite \pm \ biotite = garnet + H_2O$$

or, once epidote had reacted out

chlorite + quartz + plagioclase
$$\pm$$
 muscovite
 \pm biotite = garnet + H₂O.

The original extent of the garnet crystal has been inferred in two ways. As indicated in Fig. 3b, there is a textural and assemblage change $\sim 600 \ \mu m$ from the present garnet rim, suggesting that this marks the original rim of the garnet before resorption. The second method is to assume that the increase in Mn seen in the rim of the garnet is derived solely from the consumption of garnet by the resorption reaction. Calculation of this mass balance requires an estimate of the Mn content of the now resorbed garnet rim and Fig. 6 shows two extremes. If it is assumed that the garnet rim had constant Mn content equivalent to the minimum in the Mn zoning profile as observed in the traverses (Figs 4 & 5), then one obtains a minimum extent of the original garnet rim (Fig. 6a). Calculation with this assumption results in an inferred maximum garnet rim location that was $\sim 130 \mu m$ from the present rim.

However, it is more likely that fractionation resulted in a continuous decrease in the Mn content towards the rim (Fig. 6b) and with this assumption, one obtains a larger estimate of the original garnet size. Mass balance calculations using the model in Fig. 6b reveals that the average $X_{\rm Sps}$ concentration in the now resorbed garnet rim would have to have

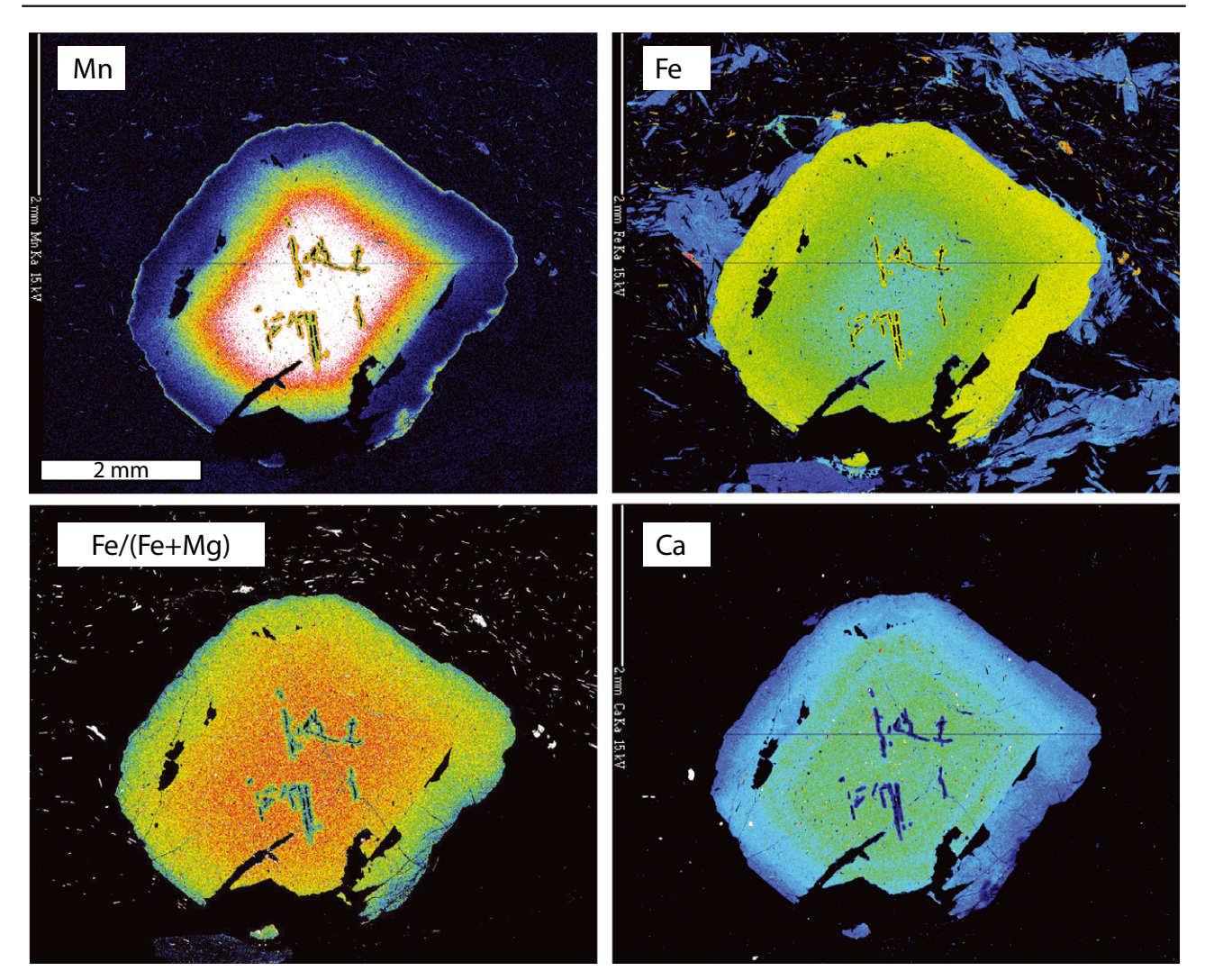


Fig. 4. X-ray maps of garnet illustrated in Fig. 3. Warmer colours denote higher values. Note monotonic decrease of Mn and Fe/(Fe+Mg) with narrow upturn at the rim. Fe increases, then decreases slightly near the rim. Ca is flat in the core and decreases towards the rim.

been around $X_{\rm Sps} = 0.0012$ to account for 600 $\mu \rm m$ of resorption (i.e. the amount indicated by the textural criteria). This is approximately half of the value of

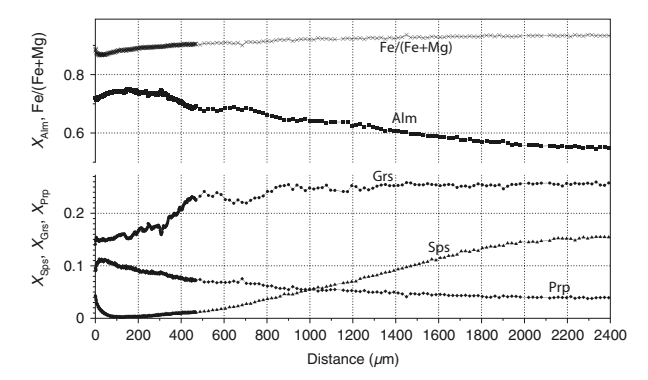


Fig. 5. Rim-to-core line traverse of garnet (see Fig. 3b for location of traverse). Point spacing was 20 μ m for the core and \sim 1 μ m for the rim.

 $X_{\rm Sps} = 0.0025$ in the minimum near the current rim, and thus the mass balance calculations appear to be consistent with the textural criteria.

In any case, the accurate position and composition of the garnet rim do not affect the results of diffusion modelling of the Mn rim to any great extent. For the models presented below, it will be assumed that the original garnet rim was $600~\mu m$ beyond the present rim and the composition was $X_{\rm Sps} = 0.0012$.

Boundary conditions

The observed zoning at the rim of the garnet provides a constraint on the boundary condition for Mn zoning as a function of garnet resorption. The measured composition of $X_{\rm Sps} = 0.044$ at the garnet rim is assumed to be the composition of the garnet rim at the time the diffusion is complete. Figure 7 shows

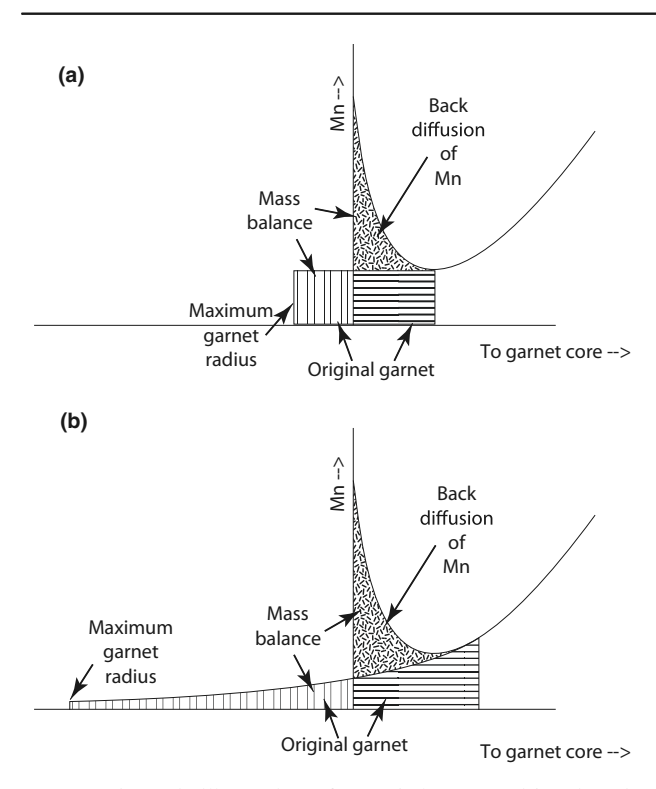


Fig. 6. Schematic illustration of mass balance considerations in estimating the extent of the initial (pre-resorption) garnet rim. (a) Assumes that the composition in the resorbed garnet rim was the same as the minimum in the Mn zoning profile and gives the minimum value for the initial garnet radius. (b) Assumes smooth zoning to the rim by fractionation. Assuming the average composition in the resorbed garnet was $X_{\rm Sps} = 0.0012$, the original garnet rim was 600 μ m beyond the present rim, consistent with the observed textural break.

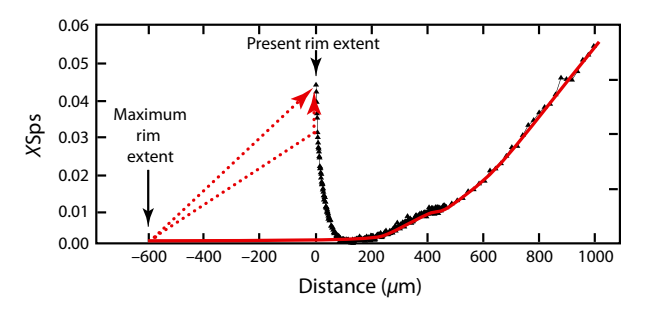


Fig. 7. Diagram of $X_{\rm Sps}$ ν . distance showing the initial conditions for modelling Mn tracer diffusion (solid red line). Dotted red lines show how the garnet rim composition changes as a function of garnet resorption for two models. Black triangles are the measured X_{Sps} profile.

two models of how the rim boundary composition was assumed to have changed as a function of garnet resorption. Both assumptions give nearly identical final durations for diffusion, but the model that involves two steps for the resorption process produces a slightly better fit for the near-rim profile. The other boundary (towards the core) is very nearly

linear and was assumed to be of fixed composition. The total linear dimension was 1600 μ m and the grid spacing $0.5 \mu m$.

RESULTS

Two model temperature—time histories were explored. The first involved instantaneous resorption of the garnet rim, a duration at the peak temperature and instantaneous cooling (i.e. a step function). The second involved linear heating to and from the peak temperature. It was assumed that resorption began 25 °C below the maximum temperature (e.g. at 575 °C for the 600 °C model) and continued monotonically to the peak temperature. Note that for both models, the initial composition profile is essentially a step function (red lines in Fig. 8) because the length scale of resorption greatly exceeds that of diffusion irrespective of the heating/cooling rate. The assumption that resorption ceased at the peak temperature rather than below it results in calculated durations being minimum estimates.

The results of the best fit models at 600 °C are shown in Fig. 8. Both models provide equally good fits to the measured Mn zoning profile. The instantaneous model provides the shortest duration of 0.8 Ma because all diffusion is assumed to have occurred at the thermal maximum. The best fit linear heating/cooling model of ± 30 °C Ma⁻¹ provides an estimate of the longest possible duration (4.3 Ma at 600 °C) because the least amount of time is spent at the thermal maximum.

To explore the sensitivity of the linear heating/ cooling model to greater durations, an experiment was run where the rate of heating/cooling was ± 20 °C Ma⁻¹. As can be seen in Fig. 8c, the diffusive penetration exceeds the measured profile by several tens of micrometres providing a degree of confidence to the maximum duration of 4.3 Ma for the 30 °C Ma⁻¹ model (Fig. 8b).

Models were run with peak temperatures of 575, 600, 625 and 650 °C (Table 1). All models resulted in fits equivalent to those shown in Fig. 8. The lower temperature models result, of course, in longer timescales with the total range for the instantaneous heating/cooling models being 0.09-2.03 Ma and for the constant heating/cooling models being 0.5–13.0 Ma.

Four-component garnet diffusion

Tracer diffusion of Mn does not accurately reflect diffusion in garnet as other cations must diffuse to maintain stoichiometry. Four-component garnet diffusion was coded in an attempt to model the zoning observed in all components on the rim of the garnet. The approach was similar to that described for Mn tracer diffusion. The initial conditions were taken to be the observed zoning in the interior of the garnet extrapolated to 600 μ m beyond the current rim. Note

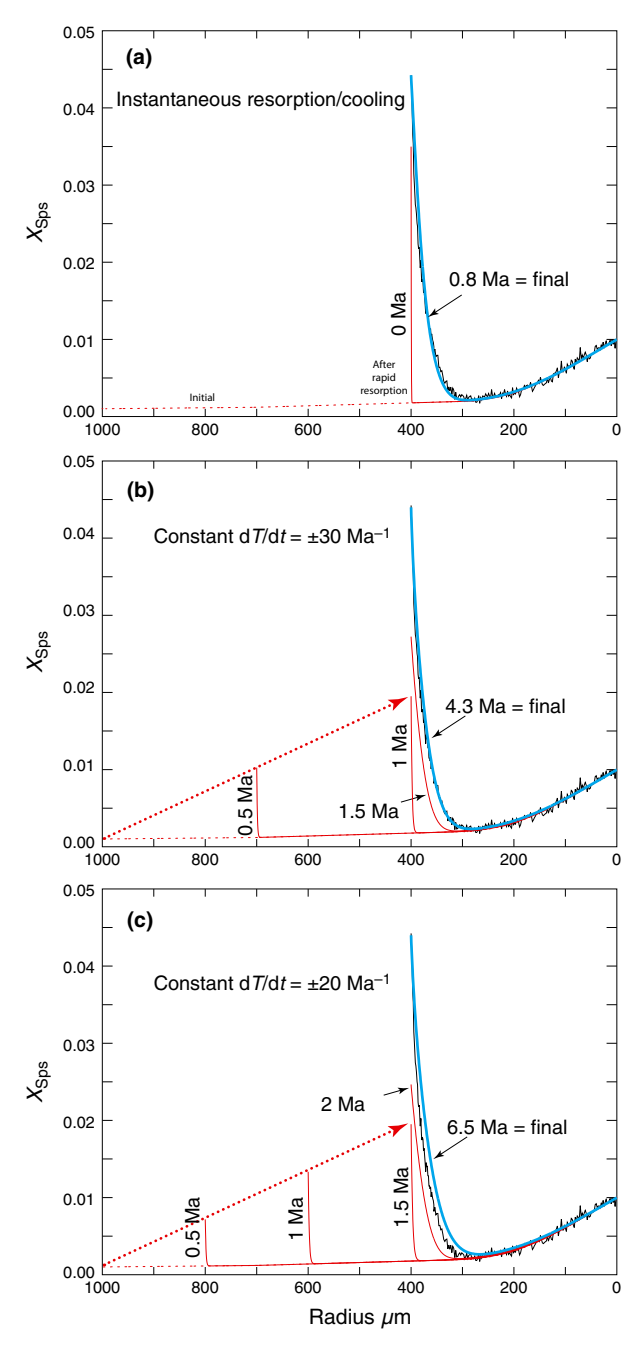


Fig. 8. Results of diffusion modelling of Mn zoning using Mn tracer diffusivity. Dotted red lines are initial conditions, solid red lines are profiles at indicated times, blue lines are final calculated profiles. Dotted lines with arrows in (b) and (c) show trajectory of garnet rim composition with reaction progress. (a) Model assuming instantaneous resorption of the rim. (b) Model assuming constant heating/cooling rate (30 °C Ma⁻¹). (c) Model assuming constant heating/cooling rate (20 °C Ma⁻¹). Note misfit of solution in (c), which places an upper limit on the duration.

that as before, the composition of the extrapolated rim does not affect the duration of the diffusion process. Magnesium was taken to be the dependent compositional parameter. The same two models were run – instantaneous and constant heating/cooling. Both models result in compositional steps at the garnet rim when resorption was complete (Fig. 9 – red line). Many tens of models were run with variations in the temperature-time history and garnet rim composition until the final result as shown in Fig. 9 (blue line) was obtained. Although other phases in the resorption reaction also contain Fe, Mg and Mn that might affect the boundary composition of garnet as the reaction proceeds (i.e. chlorite and biotite), it was determined through iterative modelling attempts that the exact garnet rim composition during the resorption process had little effect on the calculated duration of the diffusion because most of the time dependence is governed by the length scales of diffusive penetration, which is governed by the magnitude of the diffusivity (and thus the peak temperature through the Arrhenius relationship).

The four-component garnet model fits the observed zoning as well as the Mn tracer model for Mn diffusion and nearly as well for Fe and Mg diffusion. Diffusion of Ca was not sufficiently pronounced to cause much variation. The match of Fe and Mg zoning also results in a good match for Fe/(Fe+Mg) zoning.

Temperature–time plots for the instantaneous and constant heating/cooling models are plotted in Fig. 10. Note that for either set of models, the duration of the event increases exponentially with decreasing peak temperature. Total durations for diffusion for the instantaneous and constant heating/cooling models (Table 2) are very similar to those for the Mn tracer diffusion model albeit slightly longer due to the fact that Mn is the fastest diffusing species and Mn diffusion is limited by the diffusivities of other cations. Nevertheless, the durations are relatively short – <1 to <5 Ma for all but the constant heating/cooling model at 575 °C.

ESTIMATION OF PEAK TEMPERATURE

The results in Figs 8 and 9 demonstrate that good fits between the observed and modelled zoning are relatively simple to achieve. The values in Tables 1 and 2 indicate that the greatest uncertainty in the duration of the diffusion process is the inferred peak temperature. As a general observation, a change in the peak temperature of 25 °C results in a change in the diffusion time-scale by a factor of 2–3.

Estimating the peak metamorphic temperature is not straightforward using any thermometry involving garnet because the rim of the garnet is no longer available for analysis. A traditional approach to estimating peak metamorphic temperature in a sample with garnet zoning that shows an upturn in Fe/(Fe+Mg) at the garnet rim is to couple the minimum Fe/(Fe+Mg) value along the zoning profile with the composition of biotite in the sample, with the assumption that the upturn in Fe/(Fe+Mg) at the rim

Table 1. Durations for best-fit models of Mn tracer diffusion at different temperatures assuming instantaneous and constant heating/cooling.

Peak temperature	575 °C	600 °C	625 °C	650 °C
Instantaneous heating/cooling	2.03 Ma	0.69 Ma	0.27 Ma	0.09 Ma
Constant heating/cooling	13.0 Ma (±10 °C Ma ⁻¹)	4.33 Ma (±30 °C Ma ⁻¹)	1.25 Ma (±100 °C Ma ^{−1})	0.50 Ma (±250 °C Ma ⁻¹)

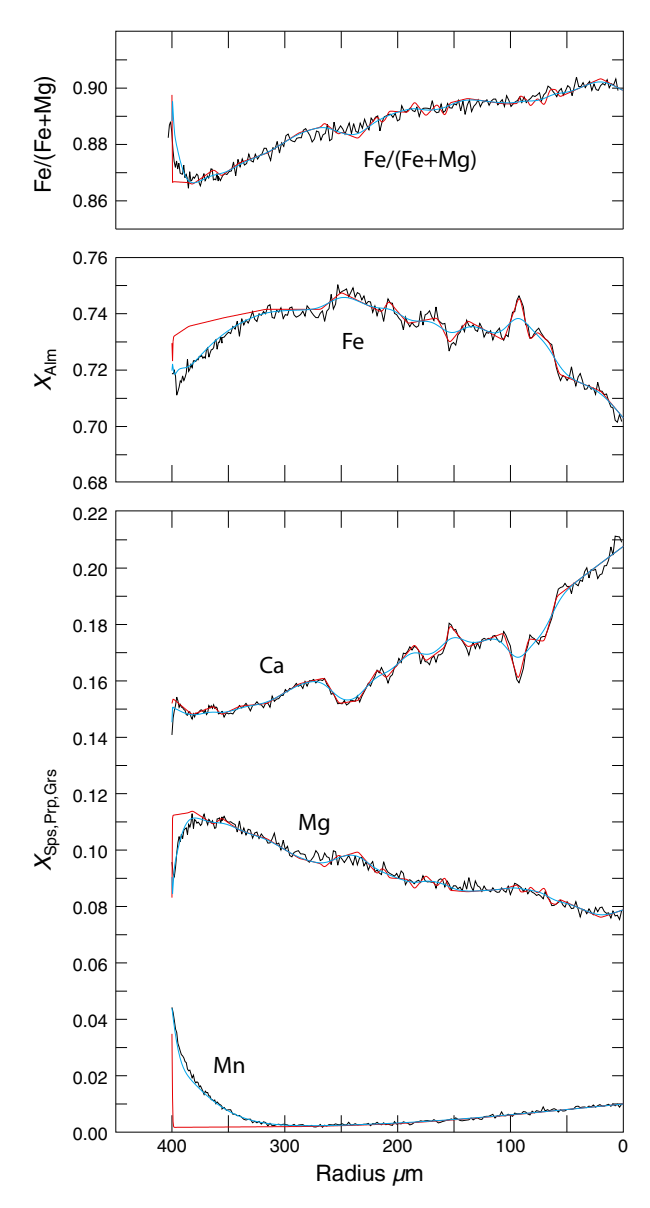


Fig. 9. Plot of radius v. composition for four-component garnet diffusion model. Black line is observed zoning 400 μ m from the rim. Red line is initial condition following garnet resorption. Blue line is the final profile. Mg was taken as the dependent compositional parameter.

is due to late-stage diffusion. Biotite in sample TM-730 displays a range of Fe/(Fe+Mg) from 0.386 to 0.466. The Fe/(Fe+Mg) map (Fig. 11) reveals no obvious core—rim or proximity to garnet pattern to the biotite composition. Plagioclase is not very

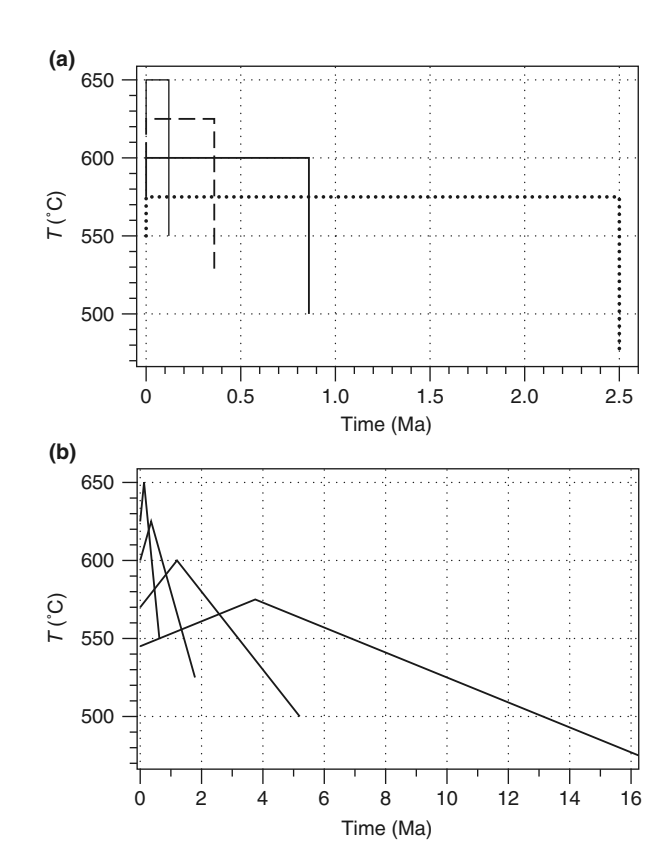


Fig. 10. Temperature—time plots for (a) instantaneous and (b) constant dT/dt four-component diffusion models. Note difference in time-scales in (a) and (b).

abundant. A grain adjacent to garnet in the reaction zone ranges in composition from An_{15} to An_{21} .

Garnet-biotite thermometry using the minimum Fe/(Fe+Mg) = 0.868 in garnet coupled with the range of Fe/(Fe+Mg) in biotite and garnet-plagioclase-kyanite-quartz barometry using the garnet rim composition ($X_{Grs} = 0.147$) and the range of plagioclase compositions yield lines of constant Keq shown in Fig. 12. The range in calculated pressure is ~1.8 kbar and the maximum temperature (at 10 kbar) is 563 °C.

It is not believed that this reflects accurately the peak metamorphic temperature. First, the upturn of the Fe/(Fe+Mg) zoning profile at the garnet rim clearly indicates that diffusion has modified the rim composition. Spear (1991) demonstrated that Fe-Mg exchange between garnet and biotite in rocks containing staurolite could, when using the 'well' in Fe/(Fe+Mg) at the garnet rim, result in inferred

Table 2. Durations for best-fit models of four-component garnet diffusion at different temperatures assuming instantaneous and constant heating/cooling.

Peak temperature	575 °C	600 °C	625 °C	650 °C
Instantaneous heating/cooling	2.5 Ma	0.86 Ma	0.36 Ma	0.12 Ma
Constant heating/cooling	16.25 Ma (±8 °C Ma ⁻¹)	5.2 Ma (±25 °C Ma ⁻¹)	1.78 Ma (±70 °C Ma ⁻¹)	0.62 Ma (±200 °C Ma ⁻¹)

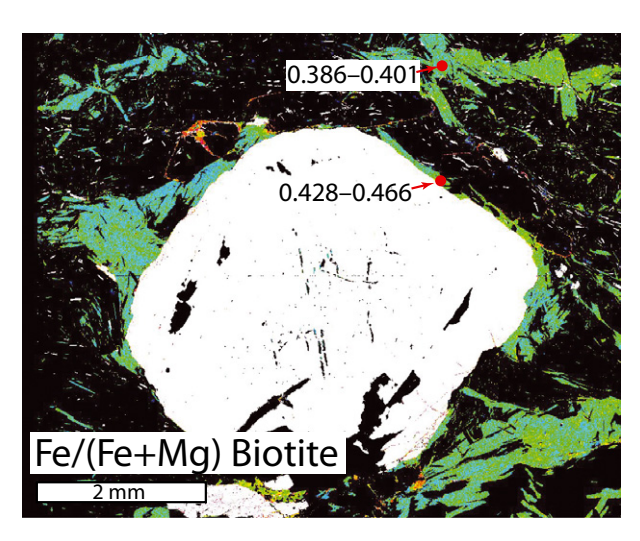


Fig. 11. Computed image enhanced to show Fe/(Fe+Mg) in biotite derived from Fe and Mg measured X-ray maps. Values show range of Fe/(Fe+Mg) at two analysis spots (red spots).

temperatures that are 70 °C below the true peak temperature, even at cooling rates as high as 100 °C Ma⁻¹. Furthermore, it is clear from the observations discussed above that a net transfer reaction has resorbed the garnet rim, clearly destroying any evidence of the garnet composition near the peak temperature.

Two approaches have been pursued to constrain the peak temperature of sample TM-730. The first involves using petrogenetic grids to infer the P-T conditions of the peak mineral assemblage (garnet + biotite + kyanite + muscovite + plagioclase + quartz \pm staurolite). The second involves forward modelling of reaction progress to help constrain the composition of the resorbed garnet rim to use in conventional thermobarometry.

Figure 12 shows a portion of the petrogenetic grid for pelites in the KFMASH system plus displacements of the grid for different compositions of garnet in the MnNCKFMASH system. The garnet composition for the heavy dotted curve ($X_{\rm Sps}=0.04$, $X_{\rm Grs}=0.15$) is representative of the garnet composition at the resorbed rim (see Fig. 5). The light dotted curves are offsets indicative of the garnet rim at maximum radius just prior to resorption. The value of $X_{\rm Sps}$ on these curves is set to 0.001 (effectively 0.0) as evaluated above with reference to Fig. 6. The extrapolated value of $X_{\rm Grs}$ at the maximum radius rim

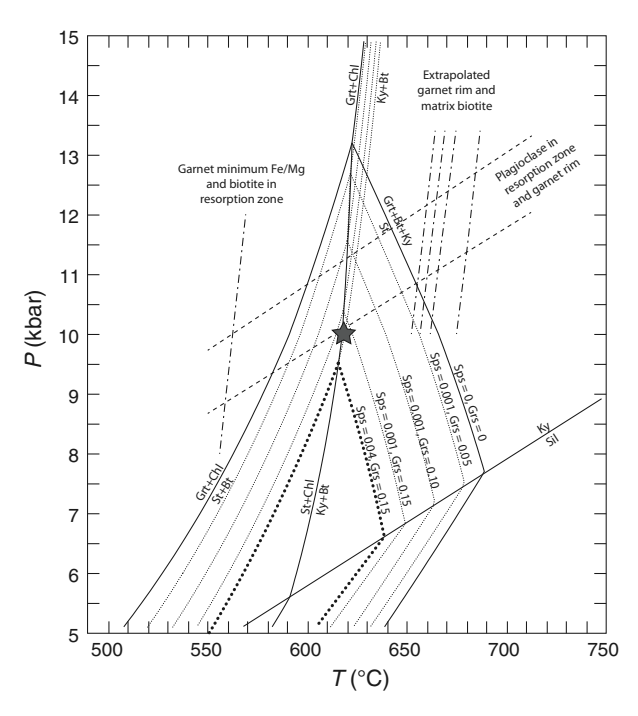


Fig. 12. *P*–*T* diagram showing a portion of the petrogenetic grid for metapelites. Black curves are KFMASH system; dotted curves are MnNCKFMASH system with garnet composition constrained as indicated; heavy dotted curve is MnNCKFMASH system with garnet composition of the resorbed rim (Sps = 0.04; Grs = 0.15). Star shows minimum temperature of kyanite + biotite association at 10 kbar. Dotdashed lines are garnet–biotite Fe–Mg thermometry using matrix biotite and extrapolated garnet rim composition and biotite in resorption zone and minimum measured Fe/Mg. Dashed lines are GASP barometry using plagioclase in the resorption zone and garnet rim composition. All assemblages contain quartz + H₂O + muscovite + biotite + plagioclase (MnNCKFMASH only).

position is less certain. Visual extrapolation (dotted curve, Fig. 13) suggests that $X_{\rm Grs}$ was ~0.135 at the maximum rim position. The results of the forward modelling (dotted and dashed curves, Fig. 13, see Discussion below) suggest that the rim composition could have been as low as $X_{\rm Grs} = 0.02$ –0.06. Because of this uncertainty, the grids in Fig. 12 have been shown at $X_{\rm Grs} = 0.0, 0.05, 0.10$ and 0.15.

The petrogenetic grids reveal that the association kyanite + biotite (the assemblage in the resorption zone) is not stable until \sim 620 °C, regardless of the bulk composition (star in Fig. 12). Note also that given the visually extrapolated $X_{\rm Grs}=0.135$ value at the maximum garnet radius, the reaction

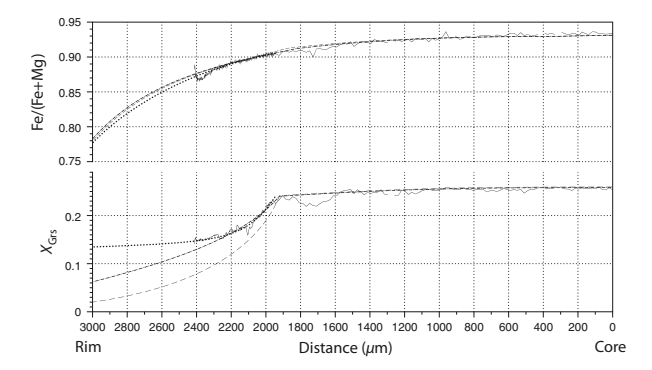


Fig. 13. Garnet composition v. radius showing different methods of extrapolation of garnet composition to the maximum radius. Dotted curves are visual extrapolation using the outer $400~\mu m$ zoning profile. Dashed and dot–dashed curves are extrapolations based on forward modelling of garnet growth using different amounts of plagioclase. Dot–dashed curves use ~5 modal per cent plagioclase; dashed curves use ~25 modal per cent plagioclase.

garnet + chlorite = staurolite + biotite will not occur until \sim 610 °C. The abundance of staurolite in various parts of this sample (see Fig. 2) indicates that this reaction was not overstepped to the extent that the stability field of staurolite was exceeded entirely. Note that the staurolite field expands as the amounts of spessartine and grossular components in the garnet decrease such that reaction within the staurolite stability field would be favoured by a lower rim $X_{\rm Grs}$ (e.g. 0.1 or 0.05).

Regardless of the rim composition of garnet at its maximum radius, as the outer 600 μ m of garnet is consumed, Mn and Ca are released into the local bulk composition such that the garnet rim composition at the cessation of resorption was around $X_{\rm Sps} = 0.04$ and $X_{\rm Grs} = 0.15$, as seen in the zoning profiles (Fig. 5). This local bulk composition is reflected in the grid in Fig. 12 by the heavy dotted curves. In the absence of any change in pressure or temperature, this change in local bulk composition would move the garnet rim environment out of the staurolite stability field and into the stability field of garnet + kyanite + biotite. That is, consumption of the garnet rim acts as a form of 'internal metasomatism' that shifts the bulk composition (cf. Spear, 1988). It is believed that this is the reason staurolite is abundant in parts of the sample (Fig. 2), but only kyanite is observed in the garnet resorption zone.

This internally consistent paragenesis indicates that the minimum temperature for garnet resorption was ~620 °C.

It might be asked why a petrogenetic grid rather than an equilibrium assemblage diagram (i.e. 'pseudosection') was used for this analysis. The answer is simple. The reactive bulk composition at any point in the rock's history is very poorly known. On the other hand, we know, or at least can constrain within limits, the composition of the garnet at

various points in the paragenesis. The petrogenetic grid is valid for all bulk composition and thus leads to a more certain interpretation than any suite of equilibrium assemblage diagrams.

The second method utilized involves calculating forward models of garnet growth with fractional crystallization similar to those reported by Spear (1988) and Spear et al. (1990). These types of models are possible using an initial measured bulk composition and modifying the bulk composition in relation to the amount and composition of garnet produced (e.g. Gaidies et al., 2008). However, the approach followed here is that described by Spear et al. (1990), which involves specifying an initial mineral assemblage calculated to be in equilibrium at the garnet isograd and then using the method of differential thermodynamics (i.e. the Gibbs method; Spear & Menard, 1989) to track changes in mineral composition and modal amount. Garnet fractionation is controlled simply by resetting the modal amount of garnet to 0 after each iteration. Numerous models were run to explore the effects of different initial conditions. As has been discussed in previous papers (e.g. Spear et al., 1990; Spear, 1993), Fe/(Fe+Mg) in garnet in the assemblage garnet + chlorite + biotite is largely controlled by changes in temperature (i.e. the isopleths are nearly vertical). Spessartine content of garnet is controlled by fractional crystallization coupled with P-T-X phase relations (e.g. Spear, 1993). Grossular content in the presence of clinozoisite or epidote is relatively constant at a value of ~0.25 (e.g. Menard & Spear, 1994) as is observed in sample TM-730 (Fig. 5). Once epidote reacts out, X_{Grs} declines through equilibria with plagioclase and the amount by which X_{Grs} declines is a function of the amount of plagioclase present.

Models were run, therefore, with the starting assemblage garnet + chlorite + biotite + muscovite + epidote + plagioclase + quartz + H_2O . The magnitude of the rock volume under consideration was adjusted to produce the observed radius of garnet prior to resorption (3 mm). Epidote was removed from the assemblage when the garnet radius reached \sim 1.9 mm, consistent with the decline in X_{Grs} seen in the zoning profiles (e.g. Figs 5 & 13).

All models produced similar changes in Fe/(Fe+Mg) with garnet radius (Fig. 13). Fe/(Fe+Mg) decreases monotonically and nearly linearly with increasing temperature and volume of garnet produced and so defines a concave downward curve due to the cube relation between volume and radius. At the maximum extent of the garnet radius (3 mm), the models provide an estimate of Fe/(Fe+Mg) that is similar to that obtained from visual extrapolation: Fe/(Fe+Mg) = 0.78. The grossular models are sensitive to the amount of plagioclase present, and the calculated zoning profiles do not match the curve deduced from visual inspection very well (Fig. 13). It is possible that an additional calcic

phase was present that was not included in the models. For example, cores of epidote crystals may have contained allanite that continued to break down via continuous reaction. However, no evidence of this was observed.

The extrapolated garnet rim compositions can be coupled with biotite analyses to infer a near-peak temperature. Only the matrix biotite composition with the lower Fe/Mg was used because the biotite in the reaction zone was not present when the garnet was at maximum radius. The resulting temperature at 10 kbar is 652-675 °C. This is higher than the minimum temperature inferred from the petrogenetic grids. Indeed, the temperature is a bit too high for garnet resorption by the reaction chlorite = kyanite + biotite even in the KFMASH system (e.g. Fig 12). However, it cannot be certain that the matrix biotite did not alter composition during resorption towards more Fe-rich compositions as would be expected during garnet resorption. These must therefore be taken as maximum temperatures for the metamorphic peak and development of the diffusional zoning profiles.

DISCUSSION

Figure 12 summarizes the various estimations of metamorphic temperatures. The petrogenetic grid adjusted for garnet composition is consistent with the peak temperature lying at or above 620 °C. Thermometry using matrix biotite and the extrapolated garnet rim composition is consistent with a peak temperature of 650–670 °C. Both of these estimates are considerably higher than the temperature of ~565 °C estimated from the minimum in Fe/(Fe+Mg) measured in garnet and reinforces the arguments of Spear (1991) about the difficulty in recovering peak metamorphic temperature in amphibolite facies metapelites.

Accepting that the peak temperature of sample TM-730 lies between 620 and 660 °C, the results of the diffusion modelling in Table 2 suggest that the time-scale for the metamorphic 'event' was in the order of 0.12–1.8 Ma, depending on the absolute temperature and the type of model chosen. Instantaneous heating and cooling is not considered likely, although it provides a limit to the shortest times. Constant heating and cooling is more realistic, and provides an upper bound to the time-scale. The actual temperature–time curve is more likely a function similar to a Gaussian curve in shape, which would yield a time intermediate between these values.

Uncertainties in the metamorphic time-scale stem from uncertainties in the peak temperature and the shape of the temperature-time curve as discussed above. An additional source of uncertainty is the values of the garnet diffusion coefficients. The diffusivities from Chakraborty & Ganguly (1992), used in this study, carry sizeable uncertainties in the temperature

range of this study (575–650 °C) because of the large extrapolation of the diffusivities from the experimental conditions of 1300–1480 °C. To evaluate the effect of this uncertainty, values of the activation energy were changed within their stated $\pm 1\sigma$ uncertainties and the value for D_0 adjusted to be consistent with the centroid of the experiments. Model diffusion calculations were then run using the four-component diffusion model at 625 °C using these 'slow' and 'fast' diffusivities. The results (Table 3) are predictably longer and shorter, respectively, than the standard values by ~ 1 order of magnitude in either direction. For example, the constant heating and cooling model requires a duration of only 0.16 Ma using the 'fast' data as compared with 1.78 Ma using the 'standard' data.

Comparison with Ti diffusion in quartz

Spear et al. (2012) published the results of diffusion modelling of Ti diffusion in quartz inclusions in garnet from samples from the same area in eastern Vermont (Fig. 1) and the time-scales are compared with the results of this study in Table 4. The data are ordered according to estimates of peak metamorphic temperature and it is clear that the duration is directly a function of the inferred peak temperature. There is broad agreement between the two independent sets of results in that both quartz and garnet diffusion models yield durations in the range of 0.1–3.0 Ma. Unfortunately, no single sample contains both quartz inclusions in garnet and such a well-defined resorption zone so that direct comparison of the two methods in the sample has not been possible. Nevertheless, the samples all come from the same regional metamorphic terrane and it is suspected, based on the analysis of sample TM-730 above, that estimates of the peak tempera-

Table 3. Durations for best-fit models of four-component garnet diffusion at 625 °C assuming instantaneous and constant heating/cooling.

	Slow	Standard	Fast
Instantaneous heating/cooling	3.5 Ma	0.51 Ma	0.05 Ma
Constant heating/ cooling	17.8 Ma (±7 °C Ma ⁻¹)	1.78 Ma (±70 °C Ma ⁻¹)	0.16 Ma (±800 °C Ma ^{−1})

Table 4. Comparison of times-scales from Ti diffusion in quartz (Spear *et al.*, 2012) with this study.

Sample	Peak T (°C)	Duration (Ma)
Garnet diffusion		
TM-730 (this study)	660 (max)	0.6
TM-730 (this study)	620 (min)	1.6
Ti in quartz diffusion		
TM-732	595	0.10
TM-828a	575	0.52
TM-543	555	0.65
09SD08A	550	1.62
TM-763	550	2.75

tures of many of the samples may be too low and that the durations inferred from models of Ti diffusion in quartz may be too long in several cases.

It is equally apparent that were the Ti diffusion calculations done at the same temperatures as the garnet diffusion calculations (for example, 625 °C), the Ti diffusion models would result in durations that are considerably shorter than those inferred from the garnet diffusion calculations. For example, the estimated peak temperature of sample TM-732 is 595 °C and were the Ti diffusion calculations to be done at 625 °C, the duration would be only in the order of 0.05 Ma. It is possible to make this inference without doing the calculations because it was determined in both this study and that by Spear et al. (2012) that the duration changes by around a factor of 2 for every 25 °C temperature change. Consequently, it appears that Ti diffusion in quartz yields significantly shorter time-scales than does cation diffusion in garnet. The reason is not clear, but it must be remarked again that the extrapolation of the Chakraborty & Ganguly (1992) data from the experimental conditions (1300–1480 °C) to the temperatures of interest (575–650 °C) is large. A possible reconciliation is manifest in the uncertainties in the garnet diffusion activation energies. Using the 'fast' model (Table 3), one obtains results that are nearly identical to those obtained from the Ti diffusion models. Whereas it is true that Carlson's (2006) very elegant analysis reconciled a number of discrepancies in garnet diffusion data, his study required assumptions about the peak temperatures and cooling histories of the samples analysed. It is, at the very least, circular to assume cooling histories in one suite of samples to obtain heating/cooling histories in another. It is also possible that some of the disagreement can be reconciled through consideration of uncertainties in the Cherniak et al. (2007) data. However, the uncertainty in the activation energy reported by these authors is only $\pm 12 \text{ kJ mol}^{-1}$ and the experiments were run at temperatures as low as 648 °C, so only minor extrapolation is required.

Comparison with geochronology

Wing et al. (2003) published SIMS ages of metamorphic monazite from the vicinity of the Strafford dome, Vermont, near sample TM-730 (see Fig. 1 for location of monazite samples and age ranges). The average age of two samples from either side of the dome is 353 Ma (± 11.8 SD and ± 2.7 SE). Individual ages have stated errors of ± 6 Ma. Figure 14 is a plot of metamorphic temperature ν . age with the metamorphic time-scales deduced in this study adjusted so that the peak temperature corresponds to the average monazite age. This adjustment is justified because, as discussed by Wing et al. (2003), the occurrence of metamorphic monazite coincides with staurolite and/or kyanite isograds and, consequently, should have

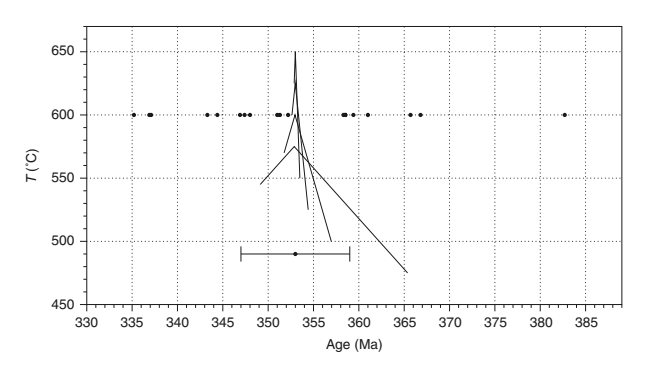


Fig. 14. Plot of temperature v. age for the study area. Dots are ages of two samples of metamorphic monazite reported by Wing *et al.* (2003) set at 600 °C to roughly coincide with the staurolite/kyanite isograd. Dot with error bars plotted at 490 °C is average age and 1σ error (353 \pm 6 Ma). Inverted 'V' curves are T-t histories from diffusion models assuming different peak temperatures (Fig. 10b) adjusted so that the peak temperature coincides with the average monazite age.

formed at approximately the same conditions as the formation of the resorbed garnet rim. It is readily apparent from the plot that the duration of the metamorphic 'event' is short relative to the spread in monazite ages and even relative to the precision of a single analysis. This observation clarifies why it has been difficult to discern the fine temporal scale of metamorphic processes except in the very youngest orogenic belts.

TECTONIC IMPLICATIONS

This study reveals a surprisingly short time-scale for the Devonian Acadian metamorphic event in Vermont. It should be made clear that these time-scales are only over the duration where significant garnet diffusion occurs – essentially within 100 °C of the peak temperature. It is suspected that rocks might reside at mid-crustal conditions for significant lengths of time prior to or following the peak metamorphic 'excursion'.

The cause of these rapid excursions is unclear. The classic analysis of Barrovian metamorphism by England & Thompson (1984) implies time-scales for metamorphic episodes in the order of tens of millions of years based on heat flow calculations of thickened crust. However, there are a number of recent studies that also suggest relatively short time-scales (e.g. Dachs & Proyer, 2002; Ague & Baxter, 2007; Viete et al., 2011). Ague & Baxter (2007) attributed the rapid thermal pulse they discovered in the Dalradian to heat input from mafic magmas. Such a scenario is not in evidence in central Vermont, which is devoid of voluminous mafic rocks of appropriate age.

It is possible to achieve short thermal pulses in a nappe complex by tectonic processes (e.g. Spear, 2011). This mechanism requires tectonic transport rates be rapid (in the order of 10 cm year⁻¹) and that

exhumation immediately follow burial so that little time for heating at depth is allowed. Furthermore, it is necessary that the tectonic slices are not overly thick (e.g. <3–5 km thick) lest the time-scale for heating by conduction be too large. If it is true that tectonic slicing is the cause of rapid metamorphic excursions in regional Barrovian terranes, then evidence of discontinuities should be apparent within the geological section. These would be difficult to observe in a heavily vegetated region such as New England, but might be apparent in a better exposed terrane. It might also be possible to infer discontinuities in metamorphic conditions or durations by detailed across-strike studies. Such work is in progress.

ACKNOWLEDGEMENTS

This work was supported by a grant from the National Science Foundation (1321777 to Spear) and the Edward P. Hamilton Distinguished Science Professor Chair (to Spear). The author thanks D. Viete and an anonymous reviewer for constructive comments.

REFERENCES

- Ague, J.J. & Baxter, E.F., 2007. Brief thermal pulses during mountain building recorded by Sr diffusion in apatite and multicomponent diffusion in garnet. *Earth and Planetary Science Letters*, **261**, 500–516.
- Carlson, W.D., 2006. Rates of Fe, Mg, Mn, and Ca diffusion in garnet. *American Mineralogist*, **91**, 1–11.
- Chakraborty, S. & Ganguly, J., 1992. Cation diffusion in aluminosilicate garnets experimental determination in spessartine–almandine diffusion couples, evaluation of effective binary diffusion coefficients, and applications. *Contributions to Mineralogy and Petrology*, 111, 74–86.
- Cherniak, D.J., Watson, E.B., & Wark, D.A., 2007. Ti diffusion in quartz. *Chemical Geology*, **236**, 65–74.
- Crank, J., 1975. The Mathematics of Diffusion. Oxford University Press, London.
- Dachs, E. & Proyer, A., 2002. Constraints on the duration of high-pressure metamorphism in the Tauern Window from diffusion modelling of discontinuous growth zones in eclogite garnet. *Journal of Metamorphic Geology*, **20**, 769–780.
- Doll, C.G., Cady, W.M., Thompson, J.B. & Billings, M.P., 1961. Centennial Geologic Map of Vermont. Vermont Geological Survey, Montpelier, Vermont.
- England, P.C. & Thompson, A.B., 1984. Pressure–temperature–time paths of regional metamorphism, Part I: heat transfer during the evolution of regions of thickened continental crust. *Journal of Petrology*, **25**, 894–928.
- Gaidies, F., De Capitani, C. & Abart, R., 2008. THERIA_G: a software program to numerically model prograde garnet growth. *Contributions to Mineralogy and Petrology*, **155**, 657–671.
- Hodges, K.V. & Spear, F.S., 1982. Geothermometry, geobarometry and the Al₂SiO₅ triple point at Mt. Moosilauke, New Hampshire. *American Mineralogist*, **67**, 1118–1134.
- Hollister, L.S., 1966. Garnet zoning: an interpretation based on the Rayleigh fractionation model. *Science*, **154**, 1647–1651.

- Kretz, R., 1983. Symbols for rock-forming minerals. American Mineralogist, 68, 277–279.
- Lasaga, A.C., 1979. Multicomponent exchange and diffusion in silicates. Geochimica et Cosmochimica Acta, 43, 455–469.
- Menard, T. & Spear, F.S., 1993. Metamorphism of calcic pelitic schists, Strafford Dome, Vermont: compositional zoning and reaction history. *Journal of Petrology*, **34**, 977–1005.
- Menard, T. & Spear, F.S., 1994. Metamorphic *P-T* paths from calcic pelitic schists from the Strafford Dome, Vermont. *Journal of Metamorphic Geology*, **12**, 811–826.
- Spear, F.S., 1988. Metamorphic fractional crystallization and internal metasomatism by diffusional homogenization of zoned garnets. *Contributions to Mineralogy and Petrology*, **99**, 507–517.
- Spear, F.S., 1991. On the interpretation of peak metamorphic temperatures in light of garnet diffusion during cooling. *Journal of Metamorphic Geology*, **9**, 379–388.
- Spear, F.S., 1993. *Metamorphic Phase Equilibria and Pressure-Temperature-Time Paths*. Mineralogical Society of America, Washington, DC.
- Spear, F.S., 2004. Fast cooling and exhumation of the Valhalla Metamorphic Core Complex. *International Geology Review*, **46**, 193–209.
- Spear, F.S., 2011. Prograde *P-T* paths: how steep, how fast, and what they mean. *American Geophysical Union Annual Meeting Abstracts*, **2011**, V13G-01.
- Spear, F.S. & Florence, F.P., 1992. Thermobarometry in granulites: pitfalls and new approaches. *Journal of Precambrian Research*, **55**, 209–241.
- Spear, F.S. & Menard, T., 1989. Program GIBBS: a generalized Gibbs method algorithm. American Mineralogist, 74, 942–943.
- Spear, F.S. & Pyle, J.M., 2010. Theoretical modeling of monazite growth in a low-Ca metapelite. *Chemical Geology*, 273, 111–119.
- Spear, F.S., Kohn, M.J., Florence, F. & Menard, T., 1990. A model for garnet and plagioclase growth in pelitic schists: implications for thermobarometry and *P-T* path determinations. *Journal of Metamorphic Geology*, **8**, 683–696. Spear, F.S., Peacock, S.M., Kohn, M.J., Florence, F.P. & Me-
- Spear, F.S., Peacock, S.M., Kohn, M.J., Florence, F.P. & Menard, T., 1991. Computer programs for petrologic *P–T*–t path calculations. *American Mineralogist*, **76**, 2009–2012.
- Spear, F.S., Ashley, K.T., Webb, L.E. & Thomas, J.B., 2012. Ti diffusion in quartz inclusions: implications for metamorphic time scales. *Contributions to Mineralogy and Petrology*, 164, 977–986.
- Thompson, J.B. & Norton, S.A., 1968. Paleozoic regional metamorphism in New England and adjacent areas. In: *Studies of Appalachian Geology, Northern and Maritime* (eds Zen, E.-A., White, W.S., Hadley, J.B. & Thompson, J.B.), pp. 319–327. John Wiley, New York.
- Viete, D.R., Hermann, J., Lister, G.S. & Stenhouse, I.R., 2011. The nature and origin of the Barrovian metamorphism, Scotland: diffusion length scales in garnet and inferred thermal time scales. *Journal of the Geological Society of London*, 168, 115–132.
- White, W.S. & Jahns, R.H., 1950. Structure of central and east-central Vermont. *Journal of Geology*, **58**, 179–220.
- Wing, B.A., Ferry, J.M. & Harrison, M., 2003. Prograde destruction and formation of monazite and allanite during contact and regional metamorphism of pelites: petrology and geochronology. *Contributions to Mineralogy and Petrology*, **145**, 228–250.

Received 28 April 2014; revision accepted 26 June 2014.